

Dalton Transactions

Accepted Manuscript



This is an *Accepted Manuscript*, which has been through the Royal Society of Chemistry peer review process and has been accepted for publication.

Accepted Manuscripts are published online shortly after acceptance, before technical editing, formatting and proof reading. Using this free service, authors can make their results available to the community, in citable form, before we publish the edited article. We will replace this *Accepted Manuscript* with the edited and formatted *Advance Article* as soon as it is available.

You can find more information about *Accepted Manuscripts* in the [Information for Authors](#).

Please note that technical editing may introduce minor changes to the text and/or graphics, which may alter content. The journal's standard [Terms & Conditions](#) and the [Ethical guidelines](#) still apply. In no event shall the Royal Society of Chemistry be held responsible for any errors or omissions in this *Accepted Manuscript* or any consequences arising from the use of any information it contains.

ARTICLE

From rational design of organometallic precursors to optimized synthesis of core/shell Ge/GeO₂ nanoparticles[†]

Cite this: DOI: 10.1039/x0xx00000x

Received 00th January 2012,
Accepted 00th January 2012

DOI: 10.1039/x0xx00000x

www.rsc.org/

D. Matioszek,^a W.-S. Ojo,^b A. Cornejo,^b N. Katir,^a M. El Ezzi,^a M. Le Troedec,^c
H. Martinez,^c H. Gornitzka,^d A. Castel,^a C. Nayral,^b and F. Delpech^{b*}

The synthesis of germanium nanoparticles has been developed thanks to the design of novel aminoiminate germanium(II) precursors: (ATI)GeZ (with Z= OMe, NPh₂, and ATI= *N,N'*-diisopropyl-aminotroponimate) and (Am)₂Ge (Am= *N,N'*-bis(trimethylsilyl)phenyl amidinate). These complexes were fully characterized by spectroscopic techniques as well as single crystal X-ray diffraction. The thermolysis of both complexes yielded NPs which display similar features that are Ge/GeO₂ core/shell structure with a mean diameter close to 5 nm with a narrow size distribution (< 15%). Whereas the high temperatures (> 300 °C) classically reported in the literature for the preparation of germanium-based NPs were necessary for thermolysis of the complexes (ATI)GeZ, the use of amidinate-based precursors allows the preparation at unprecedented low temperature (160 °C) for the thermolytic route. As suggested by a mechanistic study, the lower reactivity of (ATI)GeZ (for which the concomitant use of high temperature and acidic reagent is required) was explained in terms of lower ring strain than in the case of (Am)₂Ge.

Introduction

Because of their unique size- and shape-dependent electronic and optical properties, semiconductor nanoparticles (NPs) have sparked a considerable interest for both fundamental and technological issues across many scientific disciplines.¹ In the context of advanced microelectronic devices, semiconductors which are compatible with silicon processing techniques are of particular importance in order to minimize the cost and number of steps required for their integration. Germanium is a prominent example of such semiconductors.² However, the lack of a simple and benign synthetic pathway has so far greatly prevented the large development of applications of Ge-based NPs.^{2,3} The majority of the strategies developed for synthesizing the Ge NPs involves physical or thin film methods but, solution-based approaches have gained much interest due to their low cost and their potential scalability.^{1,2} Two main general solution strategies exist and involve either strong reducing agents or high-temperature procedures.² For the reduction route, organoalkali and alkali metal, zintl salts and hydrides are typically used to react with germanium halides such as germanium tetrachloride. However, the potential contamination by salt by-products makes separation and purification processes, as well as surface control, more difficult.⁴ In contrast, the thermal reduction route generally generates non-polluting molecules but suffers from drawbacks existing for high temperature synthesis such as energy concerns or difficulties to get rid of high-boiling-point solvents.⁵⁻⁷ Strenuous purification procedures are then required and residual solvent cannot be totally removed, resulting in high carbon contents.⁶

An ideal case would be a low-temperature synthesis with no salt by-product, i.e. involving halide-free germanium species incorporating labile substituents. This objective raises the issue of designing precursors able to fulfill these requirements. Several authors have demonstrated that the formation of Ge⁰ NPs could be advantageously achieved through the reduction of Ge(II) whatever the chosen synthesis strategy, i.e. through the assistance of strong reducing agent such as BuLi⁸ or via thermolysis.^{3,4,9} The lower reduction potential of low valent species like Ge(II) (compared to that of Ge(IV)) favors the decomposition and thus, the access to metal NPs under milder conditions. However, these works focused on GeI₂ as Ge(II) precursor and surprisingly, few studies concentrated on the use of novel Ge precursors have been reported in the literature despite the successes encountered for other semiconductors.^{10,11} To the best of our knowledge, only Boyle *et al.* have explored the reactivity of two families of tailored germanium (II) compounds: Ge(NR₂)₂ and Ge(OR)₂, R being alkyl, aryl and silyl moieties.^{4,9,12} Unfortunately, the shape control remains unsatisfactory compared to others strategies presumably. In the case of Ge[N(SiMe₃)₂]₂, the too high lability of the Ge-N bonds was invoked to explain the low control of the NPs shape.¹² In addition in contrast to expectations, high working temperatures (> 285 °C) are still required in all cases. This brief overview of the literature shows that the reported synthesis of Ge NPs requires drastic experimental conditions.

In this paper, we describe our efforts to develop new strategies toward procedures involving soft conditions. This work relies on the design of novel Ge(II) precursors and on the understanding of the decomposition mechanism in order to

implement low temperature routes for the controlled synthesis of Ge/GeO₂ core/shell NPs.

Experimental

General procedure used for germanium (II) precursors.

All manipulations with air-sensitive materials were performed in a dry and oxygen-free atmosphere of argon by using standard Schlenk-line and glove-box techniques. Solvents were purified with the MBRAUN SBS-800 purification system except THF which was distilled upon Na/Benzophenone. NMR spectra were recorded with a Bruker Avance II 300: ¹H (300.13 MHz), ¹³C (74.48 MHz) at 298 K in C₆D₆ and/or in CD₃Cl₃. Chemical shifts are expressed in parts per million with residual solvent signals as internal reference (¹H and ¹³C{¹H}). NMR assignments were confirmed by COSY (¹H), HSQC (¹H-¹³C), and HMBC (¹H-¹³C) experiments. Mass spectra were measured with a Hewlett-Packard 5989A in the electron impact mode (70 eV). Melting points were measured with a capillary electro thermal apparatus. Elemental analyses were done on a Perkin-Elmer 2400. The germanium(II) derivatives (ATI)GeCl₂ and [(Me₃SiNC(Ph)NSiMe₃)₂Ge]³⁰ were prepared according to literature procedures.

Crystal structure analysis for 1 and 2. All data (Table 1) were collected at low temperature (193 K) using an oil-coated shock-cooled crystal on a Bruker-AXS APEX II diffractometer with Mo K α radiation ($\lambda = 0.71073 \text{ \AA}$). The structures were solved by direct phase determination (SHELXS-97)³³ and refined for all non-hydrogen atoms by full-matrix least-square methods on F^2 and subjected to anisotropic refinement.³⁴

1: C_{17.50}H₂₆GeN₂O, M = 352.99, crystal size = 0.60 x 0.20 x 0.05 mm³, monoclinic, space group P2₁/c, $a = 12.94(2) \text{ \AA}$, $b = 8.62(2) \text{ \AA}$, $c = 17.02(2) \text{ \AA}$, $\beta = 110.78(3)^\circ$, $V = 1775(4) \text{ \AA}^3$, $Z = 4$, $T = 173(2) \text{ K}$, 16863 reflections collected, 2508 unique reflections ($R_{\text{int}} = 0.0442$), $R1 = 0.0508$ [$I > 2\sigma(I)$], $wR2 = 0.1630$ (all data), residual electron density = $1.286/-0.521 \text{ e \AA}^{-3}$.

2: C₂₅H₂₉GeN₃, M = 444.10, crystal size = 0.30 x 0.10 x 0.10 mm³, orthorhombic, space group Pna2₁, $a = 21.099(2) \text{ \AA}$, $b = 8.055(1) \text{ \AA}$, $c = 12.916(1) \text{ \AA}$, $V = 2195.2(2) \text{ \AA}^3$, $Z = 4$, $T = 193(2) \text{ K}$, 22008 reflections collected, 4347 unique reflections ($R_{\text{int}} = 0.0320$), $R1 = 0.0244$, [$I > 2\sigma(I)$], $wR2 = 0.0583$ (all data), residual electron density = $0.302/-0.228 \text{ e \AA}^{-3}$.

CCDC-983765 and CCDC-983766 contain the supplementary crystallographic data. These data can be obtained free of charge from The Cambridge Crystallographic Data Centre via www.ccdc.cam.ac.uk/data_request/cif.

(ATI)GeOMe (1): A solution of *n*-BuLi (0.96 mL, 1.54 mmol) in hexane (1.60 mol/L) was slowly added to a solution of MeOH (0.06 mL, 1.56 mmol) in THF (4 mL) at -65 °C. This solution was raised at -40 °C and was slowly added to a solution of (ATI)GeCl₂ (0.43 g, 1.38 mmol) in THF (4 mL) at -78 °C. After 3h under magnetic stirring at room temperature, the volatiles were removed in *vacuo* and the residue was treated by toluene (5 mL). After filtration, the filtrate was concentrated and the resulting precipitate was washed with pentane (three times with 4 mL) to yield **1** as a red sticky product. Yield: 0.35 g (81%). M.p. 58 °C. ¹H NMR (CDCl₃): δ (ppm) = 1.42 (d, ³J_{H-H} = 6.5 Hz, 6H, (CH₃)₂CH); 1.46 (d, ³J_{H-H} = 6.5 Hz, 6H, (CH₃)₂CH); 3.20 (s, 3H, OCH₃); 4.05 (sept, ³J_{H-H} = 6.5 Hz, 2H, (CH₃)₂CH); 6.38 (t, ³J_{H-H} = 9.3 Hz, 1H, H₅); 6.55 (d, ³J_{H-H} = 11.6 Hz, 2H, H_{3,7}); 7.05 (t, ³J_{H-H} = 11.5 Hz, 2H, H_{4,6}). ¹H NMR (C₆D₆): δ (ppm) = 1.27 (d, ³J_{H-H} = 6.6 Hz, 6H, (CH₃)₂CH); 1.43 (d, ³J_{H-H} = 6.6 Hz, 6H, (CH₃)₂CH); 3.47 (s, 3H, OCH₃); 3.67 (sept, ³J_{H-H} = 6.4 Hz,

2H, (CH₃)₂CH); 6.20 (t, ³J_{H-H} = 9.3 Hz, 1H, H₅); 6.25 (d, ³J_{H-H} = 11.5 Hz, 2H, H_{3,7}); 6.73-6.80 (m, 2H, H_{4,6}). ¹³C NMR (CDCl₃): δ (ppm) = 23.36 ((CH₃)₂CH); 48.73 ((CH₃)₂CH); 50.57 (OCH₃); 112.82 (C_{3,7}); 119.83 (C₅); 136.37 (C_{4,6}); 160.09 (C_{2,8}). CI-MS (NH₃) m/z (%): [M + 1]⁺ = 309 (3%); [M - OCH₃]⁺ = 277 (100%). Elemental analysis calculated for C₁₄H₂₂N₂OGe: C, 54.78%; H, 7.22%; N, 9.13%. Found: C, 54.19%; H, 7.24%; N, 9.30%.

(ATI)GeNPh₂ (2): A solution of *n*-BuLi (1.15 mL, 1.82 mmol) in hexane (1.60 mol/L) was slowly added to a solution of Ph₂NH (0.29 g, 1.65 mmol) in diethylether (5 mL) at 0 °C. The solution was stirred for 45 minutes at room temperature and then further 20 minutes at 35 °C. This solution was slowly added to a solution of (ATI)GeCl₂ (0.49 g, 1.57 mmol) in diethylether (25 mL) at -60 °C. After 16h under magnetic stirring at room temperature, the volatiles were removed in *vacuo* and the residue was treated by toluene (4 mL). After filtration, the filtrate was concentrated and the resulting precipitate was washed with pentane (three times with 4 mL) to yield **2** as a yellow powder (0.64 g, 92%). M.p. 67 °C. ¹H NMR (C₆D₆, 298 K): δ 1.08 (d, ³J_{H-H} = 6.5 Hz, 6H, (CH₃)₂CH); 1.35 (d, ³J_{H-H} = 6.5 Hz, 6H, (CH₃)₂CH); 3.45 (sept, ³J_{H-H} = 6.5 Hz, 2H, (CH₃)₂CH); 5.99 (d, ³J_{H-H} = 11.7 Hz, 2H, H_{3,7}); 6.07 (t, ³J_{H-H} = 9.3 Hz, 1H, H₅); 6.59-6.66 (m, 2H, H_{4,6}); 6.77-6.86 (m, 4H, C₆H₅); 7.07-7.15 (m, 6H, C₆H₅). ¹³C NMR (C₆D₆, 298 K): δ 22.38 and 22.75 ((CH₃)₂CH); 48.59 ((CH₃)₂CH); 114.04 (C_{3,7}); 118.05 (C₅); 119.51 (C₆); 120.97 (C_p); 129.06 (C_m); 136.35 (C_{4,6}); 143.52 (C_i); 160.82 (C_{2,8}). CI-MS (NH₃) m/z (%): 446 (2) [M + 1]⁺; 277 (26) [M - N(C₆H₅)₂]⁺.

General procedure used for germanium nanomaterials.

All manipulations with air-sensitive materials were performed in a dry and oxygen-free atmosphere of argon by using standard Schlenk-line and glove-box techniques. 2D DOSY (Diffusion Ordered Spectroscopy) NMR spectra were recorded on a Bruker Avance 500 equipped with an inverse Z-gradient (TBI, BB) at 298 K in CDCl₃. Solid State NMR spectra were performed on a Bruker Avance 400 equipped by a 4 mm probe: ¹³C MAS (Magic angle spinning). IR spectra were measured on a Varian 640-IR FT-IR spectrometer. RAMAN spectra were recorded on a Labram HR 800 Horiba-Jobin and Yvon equipped with a HeNe laser $\lambda_{\text{exc}}=632\text{nm}$. UV-Visible absorbance spectra were acquired on a Perkin-Elmer Lambda 35 scanning spectrophotometer with the samples in 2 mm quartz cells. ThermoGravimetric Analyses (TGA) were collected on a SETARAM 92-16.18 Thermobalance under nitrogen at a temperature range of 27-600 °C with a heating rate of 10 °C/min. Ge nanomaterials samples for Transmission Electron Microscopy (TEM) were prepared in a glovebox by slow evaporation of a drop of the chloroform Ge nanomaterials solution on a TEM carbon-covered copper grid. Images were collected on a Jeol JEM-1011 apparatus (100 kV, resolution of 4.5 Å). The size distribution was determined by measuring over 300 particles. Photoluminescence analysis was recorded at 20 °C using a Xenon lamp (70 Watts) and a MD-5020PTI photomultiplier (900 V) with a 2 nm monochromator. Data were recorded with the Felix software. XPS measurements were carried out with a Kratos Axis Ultra spectrometer, using a focused monochromatized Al K α radiation ($h\nu=1486.6 \text{ eV}$). The XPS spectrometer was directly connected to an argon dry box through a transfer chamber, to avoid moisture/air exposure of the samples. For the Ag₃ d_{5/2} line the full-width at half maximum (fwhm) was 0.58 eV under the recording conditions. The analyzed area of the samples was 300 μm x 700 μm (large scale). Peak assignments were made with respect to reference compounds analysed in the same conditions. The binding energy scale was calibrated from hydrocarbon contamination using the C 1s peak at

285.0 eV. Core peaks were analysed using a non-linear Shirley-type background. The peak positions and areas were optimized by a weighted least-square fitting method using 70% Gaussian, 30% Lorentzian lineshapes.

Nanoparticle synthesis.

From (ATI)Ge(OMe) (1): In a three neck round-bottomed flask, connected to a reflux condenser and a Pt-thermal probe, was added 15 mL of octadecene (ODE). The latter was degassed for one hour under reduced pressure at 120 °C after while the temperature was allowed to be raised at 320 °C under 1 atm. A solution of (ATI)Ge(OMe) (0.05 g, 0.16 mmol) and oleic acid (0.46 g, 1.61 mmol) in mesitylene (5 mL) was directly injected into the ODE refluxing solvent. After elimination of the mesitylene by distillation, the resulting mixture was refluxed at 320 °C for 1 hour. The ODE was eliminated by distillation under reduced pressure and the particles were washed three times. In the standard procedure, the resulting yellowish oil was dissolved in chloroform (1 mL) and acetone (15 mL) was added giving a cloudy solution which was centrifuged 20 minutes (20.000 RPM). The supernatant was removed and the residue dried under reduced pressure (10^{-5} mbar) at 150 °C for 6 hours. The particles were isolated as a yellowish sticky product.

From (Am)₂Ge (3): In a three neck round-bottomed flask, were loaded (Am)₂Ge (0.06 g, 0.10 mmol), oleic acid (0.14 g, 0.50 mmol), oleylamine (2.5 g, 7.5 mmol) and mesitylene (2.5 mL). The flask was then connected to a reflux condenser and heated to 160 °C under Ar. The reaction temperature was maintained at 160 °C for 24 hours. The mesitylene was eliminated by distillation under reduced pressure and the particles were washed three times. In the standard procedure, the resulting yellowish oil was dissolved in chloroform (2 mL) and ethanol (10 mL) was added giving a cloudy solution which was centrifuged 15 minutes (20.000 RPM). The supernatant was removed and the residue dried under reduced pressure (10^{-5} mbar) at 150 °C for 24 hours. The particles were isolated as a yellowish sticky product.

Results and discussion

Our work focused on the use of chelating nitrogen-based ligands which could provide a balance between the reactivity of the Ge–N bonds and the robustness of chelating ligands. More precisely, the influence of two amino-iminate ligands was explored, the *N,N'*-diisopropylaminotroponimate (ATI) and the *N,N'*-bis(trimethylsilyl)phenylamidinate (Am) ligands.

A. Aminotroponimate-based germanium complex as Ge/GeO₂ NPs precursor.

The chelating *N,N'*-diisopropylaminotroponimate ligand (ATI) is known as a valuable ligand to allow the isolation of low valent and low coordinate Ge species.¹³ Knowing that the Ge–ligand bond strength plays a key role in the reactivity of the precursor, alkoxide and amido groups were chosen as second substituents, the first one yields to a strong Ge–O bond (dissociation energy of 80–100 kcal/mol)¹⁴ while the other one possesses a weak Ge–N bond (55 kcal/mol).¹²

Precursor synthesis and characterization. The functionalized gerylenes (ATI)GeZ (Z= OMe (1), NPh₂ (2)) were obtained in high yields by one-pot reactions of (ATI)GeCl¹⁵ with LiOMe (for 1)

and LiNPh₂ (for 2) in a 1:1 ratio in diethyl ether or THF (Scheme 1). Compounds 1 and 2 are soluble in common organic solvents and are stable in the absence of air and moisture. They were fully characterized by spectroscopic methods and their structures confirmed by single-crystal X-ray analysis as shown in Figures 1 and 2, respectively. Selected bond lengths and angle are given in Table 1.

Scheme 1. Syntheses of the ATI stabilized gerylenes 1 and 2.

The crystals of compounds 1 and 2 suitable for single-crystal X-ray diffraction studies were grown from toluene/hexane and toluene/hexane/THF solutions at -24 °C for 1 and 2, respectively. The aminotroponimate ligand chelates to the germanium center to form a planar heterobicyclic C₇N₂Ge system with the germanium atom lying 0.01 Å (in 1) and 0.15 Å (in 2) out of the plane defined by the other atoms. The germanium atom is three-coordinated and adopts a trigonal-pyramidal geometry (the sums of the angles are 270° for the two compounds) with the bonded heteroatom approximately orthogonal towards the heterobicyclic plane. The average Ge–N bond distances (1.99 Å and 1.97 Å respectively, in 1 and 2) are in the normal range of cyclic conjugated bonds (1.96 Å).¹⁵ Surprisingly, the exocyclic Ge–N distance (1.977(2) Å) in 2 is close to the values previously observed in the five-membered NGeNCC rings and longer than those found for germanium(II) amides.¹⁶ In addition, one of the N–C_{phenyl} bond distance (1.393(2) Å) is shortened when compared to the other (1.438 Å). This seems to indicate an extension of the electronic delocalization involving one phenyl ring and the nitrogen atom leading to a positive charge on the nitrogen atom and by consequence to a less strong bond between the germanium and the nitrogen atom. The Ge–O distance (1.845 Å) in 1 is quite close to those observed for alkoxygermylene (1.844 Å)^{12, 17}, for hydroxygermylene (1.840 Å)¹⁷ and is characteristic of a covalent Ge–O bond (1.82 Å).¹⁶

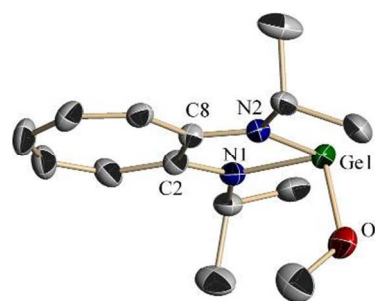


Figure 1. Molecular structure of 1 with thermal ellipsoids presented at the 50% probability level. Hydrogen atoms have been omitted for clarity.

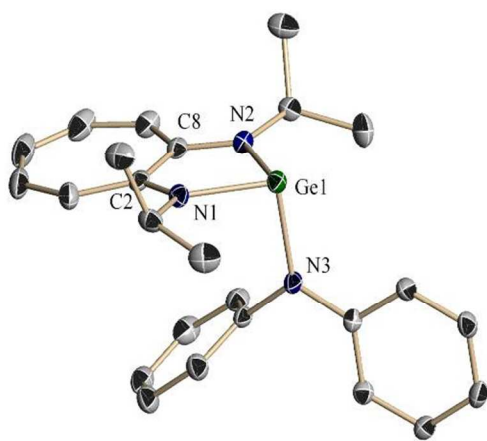


Figure 2. Molecular structure of **2** with thermal ellipsoids presented at the 30% probability level. Hydrogen atoms have been omitted for clarity.

	1	2
Ge1–N1	1.994(5)	1.964(2)
Ge1–N2	1.996(4)	1.971(2)
Ge1–N3	-	1.977(2)
Ge1–O1	1.845(5)	-
N1–C2	1.338(7)	1.331(3)
N2–C8	1.328(7)	1.330(3)
N1–Ge1–N2	78.50(19)	79.67(8)

Table 1. Selected bond lengths [Å] and angles [°] in the compounds **1-2**.

In order to gain insight into the suitability of these precursors for nanomaterials production, thermal gravimetric analyses (TGA) were performed for each compound (Figure S1). In both cases, the initiation of the organic decomposition occurred around 200 °C that is in the range of the decomposition temperature observed for germanium(II) precursors.¹²

Ge-based NPs: synthesis and characterization. NPs were prepared via thermolysis of the Ge complex (ATI)GeZ **1** and **2** at 320 °C in octadec-1-ene (ODE) in the presence of oleic acid (OIA). The use of carboxylic acid is required in order to obtain well-dispersed and size-controlled NPs (see Figure S2 for a synthesis in the absence of OIA). In a typical reaction, (ATI)Ge(OMe) and OIA are dissolved in mesitylene and injected in an ODE solution at 320 °C. The reaction mixture is, then, held at this temperature for 1 h. Synthesis run at lower temperature failed in preparing NPs. Similar results were obtained when using the germynes **1** and **2**, suggesting that the nature of the Z substituent is not central for the NPs synthesis. For sake of clarity, only those of **1** will be presented here. Figure 3 displays a typical transmission electron microscopy (TEM) image of these NPs with the energy-dispersive X-ray spectroscopy (EDX) spectrum which confirms the presence of Ge (Figure S3). The mean diameter of the roughly spherical particles is centered on 5.2(0.7) nm with a relatively narrow size distribution. The XRD pattern of the NPs was collected and found to be featureless indicating that either amorphous Ge material was obtained or, that the crystalline domains are too small to be detected by XRD.

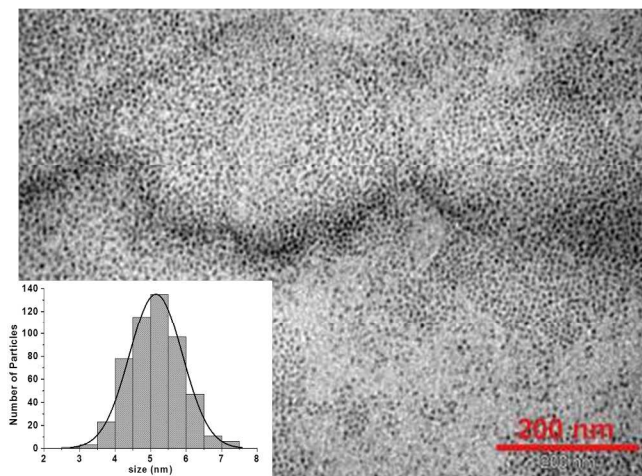


Figure 3. TEM image of germanium NPs prepared from **1** at 320°C. The inset shows the size distribution diagram.

Quantitative compositional information were obtained from several analysis methods (XPS, ICP-MS, TGA) and are consistent with the presence of a high organic content (more than 90% weight) due to the surface ligands. Additionally, XPS and Raman spectroscopy were used to probe the inorganic core (Figure 4). Raman spectroscopy is, a highly relevant method for characterizing the presence of Ge whether it is crystalline or amorphous: crystalline Ge is characterized by an intense and thin band close to 300 cm^{-1} while, in the corresponding amorphous material, the disorder changes the vibrational density of states and leads to the observation of broad bands at lower wavenumbers (150-270 cm^{-1}).^{18,19} The spectrum of the Ge NPs studied by micro-Raman analysis, is displayed in Figure 4. A broad and intense band at 215 cm^{-1} clearly shows the presence of a Ge(0) core and confirm its non-crystalline form. Moreover, weak humps of amorphous Ge oxides can be observed at 350 and 410 cm^{-1} .²⁰ Interestingly when using XPS, only signatures of amorphous Ge oxides can be evidenced: the Ge 3d core peaks are presented in Figure 4 and this spectrum shows germanium mixed oxides with characteristic peaks at (30.9 eV, 31.5 eV), (32.1 eV, 32.7 eV) and (32.9 eV, 33.5 eV) attributed to 3d_{5/2} and 3d_{3/2} peaks associated respectively to Ge(II), Ge(III) and Ge(IV) oxidation states. Given the penetration depth of XPS (approximately 6 nm) and the organic layer at the surface of the NPs, this can be interpreted as the result of the sole probing of the upper layer of the inorganic core and thus, suggest the formation of a Ge/GeO₂ core/shell structure. The formation of the oxide shell is in strong contrast with the observations made for the Ge NPs prepared from Ge[N(SiMe₃)₂]₂.⁴ In this latter case, no Ge–O bond was identified while similar reaction conditions were used (in particular similar high temperatures > 300 °C). This difference can be presumably assigned to the use in our system of carboxylic ligands (only amine was used by Boyle et al.⁴) which are known to yield the formation of an oxide shell because of side-reactions (decarboxylative coupling of carboxylic ligands at high temperatures).⁷

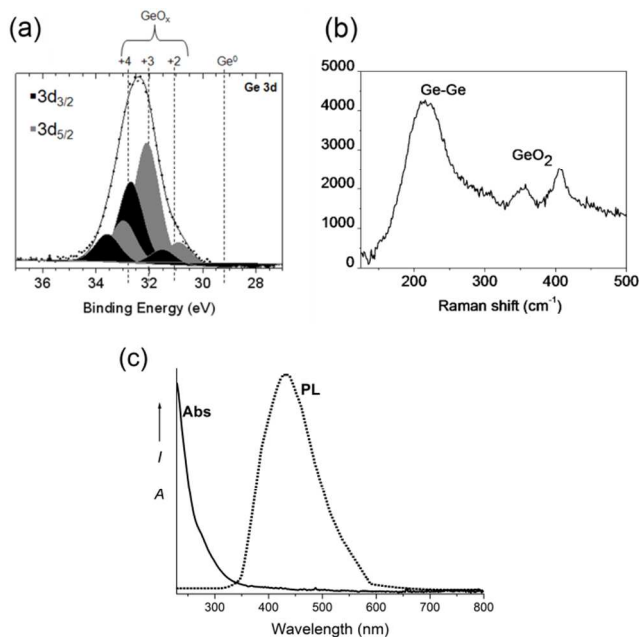


Figure 4. (a) XPS, (b) Raman and (c) UV-Vis absorption and photoluminescence spectra of germanium NPs prepared from **1** at 320 °C.

The optical properties and in particular the photoluminescence (PL) response (centred at ca. 440 nm) are consistent with the presence of both metal germanium and oxide in the NPs (Figure 4). This spectral feature can be attributed to an oxide-mediated radiative transition, and probably arises from Ge/GeO₂ surface oxide states.²¹

Surface-Ligand composition and dynamics. The key importance of the ligands and their dynamics in the synthesis and the properties of the NPs^{22,23} have stimulated us to examine the surface environment of the Ge/GeO₂ NPs. Solution and solid-state NMR techniques, which are powerful tools to probe the surface of NPs at the molecular scale,²⁴ were employed. The ¹H NMR spectrum of the Ge/GeO₂ NPs in chloroform shows well-resolved resonances of oleate as well as of residual ODE in a 1 : 2.2 ratio. Using the diffusion-ordered NMR spectroscopy (DOSY) sequence – experiment which measures the translational diffusion of the ligand – the diffusion coefficient of oleate was shown to decrease significantly compared to that of the blank OIA solution (1.7×10^{-10} m²/s vs. 6.3×10^{-10} m²/s) (Figure 5). Similarly, the one of ODE associated to the NPs is much smaller than the one of the blank solution of ODE (1.7×10^{-10} m²/s vs. 10.7×10^{-10} m²/s) (Figure 5).

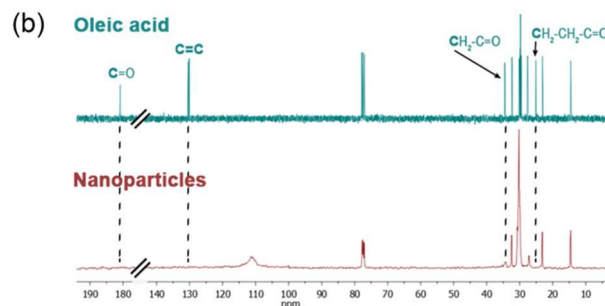
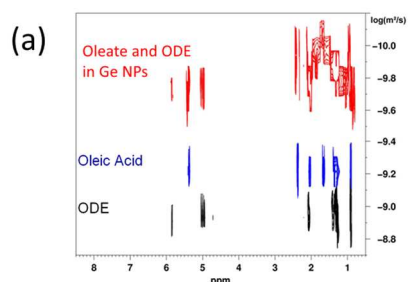


Figure 5. (a) Overlay of 2D DOSY NMR spectra, in CDCl₃, of pure oleic acid, of pure ODE and of germanium NPs prepared from **1** at 320 °C. (b) Comparison of the MAS ¹³C{¹H} NMR spectra of pure oleic acid, and of germanium NPs prepared from **1** at 320 °C.

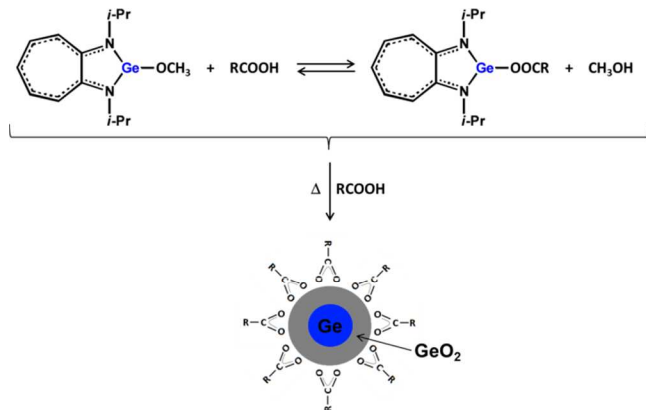
The self-diffusion coefficients and hydrodynamic radii are correlated by the Stokes-Einstein relation $D = (kT)/(6\pi\eta r)$ (where D is the diffusion coefficient, k is the Boltzmann constant, T is the temperature in K, η is the viscosity of the solution, and r is the radius). The diffusion coefficient value of 1.7×10^{-10} m²/s indicates a hydrodynamic diameter of 4.9 nm in chloroform. This value is consistent with the size measured by TEM 5.2(0.7) nm and thus, shows that the oleate ligands are tightly bound to the NPs surface. In the case of ODE, the reduction of diffusion coefficient may be more probably due to interaction via van der Waals interaction with coordinated oleate rather than direct complexation of the olefin function at the surface of the Ge NPs. Consistently the solution NMR results, the magic angle spinning (MAS) ¹³C{¹H} NMR spectrum features the vanishing and/or broadening of carbonyl, olefinic and adjacent carbons resonances (Figure 5). These effects are due to the decrease of fluxionality resulting from the coordination and/or interaction with the NPs, as previously noted when a surfactant molecule interacted with a nanoparticle surface.^{10,25,26} They also strongly support the coordination through the carboxylate moiety and the proximity of its olefin function to the surface of the NPs.

Mechanistic study of the formation of Ge/GeO₂ core/shell NPs.

When changing the stabilizing system, i.e. using the amine hexadecylamine (HDA) or a mixture of HDA and oleic acid as ligands, no NPs could be obtained. These results clearly showed that the oleic acid plays a key role which goes well beyond the only stabilization and, thus, that it must be involved in the decomposition mechanism. This result has prompted us into studying the mechanism in more detail and clarifying the precise role of oleic acid.

We, first, examined the first step of the synthesis of the NPs, i.e. the reaction of (ATI)Ge(OMe) with carboxylic acid at room temperature. The ¹H NMR spectrum in CDCl₃ (Figure S4) evidences the presence of residual (ATI)Ge(OMe) and the formation of the methanol which suggests that some of the initial Ge(II) species is converted into (ATI)Ge(OI) (OI stands for oleate). Thus, the solution which is injected at 320 °C, actually contains a mixture of germanium species. Interestingly, the presence of (ATI)Ge(OMe) is essential for the NPs formation since the sole use of (ATI)Ge(OI) (prepared separately) as precursor for the synthesis of NPs, failed in the preparation of nano-object. Then, we examined the second step of the preparation (i.e. injection at 320 °C and heating during 1h) using UV-Vis spectroscopy (Figure S5). After 5 min of reaction, the

UV-Vis spectrum of the solution was strikingly similar to that of the aminotroponimine, suggesting the release of the ATI ligand in its acid form (aminotroponimine) during the preparation of NPs. Then, the spectrum becomes gradually featureless with time, presumably because of the decomposition of the generated aminotroponimine. These observations allow us to draw the following conclusions: i) An equilibrium between two Ge(II) species ((ATI)Ge(OMe) and (ATI)Ge(OI)) exists in the reaction mixture when preparing the precursor solution before the injection (Scheme 2).



Scheme 2: Mechanism of the formation of germanium NPs from 1.

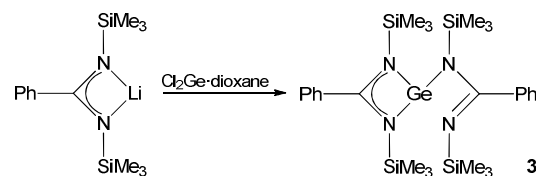
However, the presence of the first complex is required to get the Ge/GeO₂ core/shell NPs, presumably because it may allow nucleation to proceed. This result also raises the question of the role of the *in situ* generated (ATI)Ge(OI) since it decomposes during the reaction but do not yield to NPs if used alone. A plausible hypothesis is its involvement only in the growth process. ii) The use of carboxylic acid is mandatory in order to get NPs. The observation of the release of aminotroponimine by UV-Vis (Figure S5) suggests that oleic acid helps to decoordinate the strong chelating ATI ligand through the assistance of the acidic protons. In contrast, fatty amine like HDA or the mixture of fatty amine and acid, which are known to form ion pairs²⁷ may not be acidic enough to break the N-Ge-N link.

The insights provided by this mechanistic study encouraged us into designing new Ge(II) complex incorporating weaker chelating ligand forming more strained cycle such as amidinate. This latter should indeed, be easier to decoordinate and thus, allows decreasing the working temperature for softer conditions.

B. Amidinate-based germanium complex as Ge/GeO₂ NPs precursor.

The amidinate ligand was chosen on the basis of the literature reports which showed the higher reactivity of amidinate complexes compared to their counterpart incorporating aminotroponimate.^{13,28,29}

Precursor synthesis and characterization. The bis(amidinato)germylene **3** was prepared by treatment of Cl₂Ge dioxane with the lithium amidinate salt in a 1:2 stoichiometry according to the method previously described (Scheme 3).³⁰



Scheme 3: Synthesis of the bis(amidinato)germylene (Am)₂Ge (**3**).

This germanium(II) species was isolated as pale yellow powder which is stable under inert atmosphere and can be stored for long periods at low temperature (-30 °C). It is to note that the thermal decomposition temperature of **3** (150 °C) is clearly lower than those of the ATI-based germylenes and suggests a lower stability probably due to the presence of a strained four-membered cycle (Figure S1).

Ge-based NPs: synthesis and characterization. Following a similar strategy than that used with the ATI-based precursor, Ge/GeO₂ NPs were prepared successfully at 160 °C via the thermolysis of the bis(amidinate) germanium complex **3**. In a typical reaction, (Am)₂Ge, OIA and oleylamine in a 0.2 : 1 : 15 ratio are dissolved in mesitylene and heated at 160 °C for 24 h. Figure 6 displays a typical TEM image of the as-synthesized NPs which have a mean diameter of 4.7(0.6) nm.

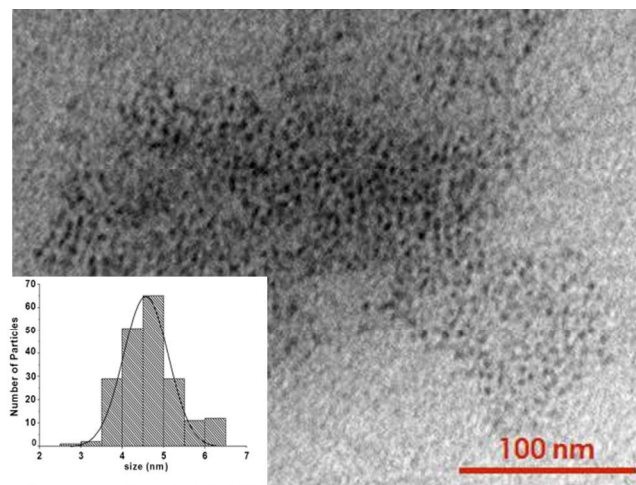


Figure 6. TEM image of germanium NPs prepared from **3** at 160 °C. The inset shows the size distribution diagram.

The full characterization (TEM, XRD, Raman, UV-Vis and PL spectroscopies) of the NPs prepared at 160 °C (Figures 6 and S6) allows showing that the obtained nano-objects are very similar to those obtained at high temperature with (ATI)Ge(OMe) or with (Am)₂Ge at 320 °C (Figures 3, 4, S6, S7). More precisely, the presence of mixed amorphous Ge/GeO_x nanoparticles was identified thanks to featureless XRD and to the Raman spectrum (Figure S6). This latter displays an intense and broad Ge-Ge band (~220 cm⁻¹) characteristic of amorphous germanium together with weaker resonances between 300 and 450 cm⁻¹ typically found in materials incorporating Ge oxides.²⁰ The presence of oxide is further supported by the PL optical signature around 400 nm as previously observed for the NPs prepared from (ATI)Ge(OMe). Optimized results in terms of size distribution (< 15%) were obtained when ligands are oleate and oleylamine (Figure 6) presumably because the association of both ligands induces a soft but robust template.²⁷ The diffusion coefficient of oleylamine determined by NMR DOSY (that of oleate could not be measured between of the large excess of

oleylamine) was similar to that of the blank ligand solution ($6.7 \times 10^{-10} \text{ m}^2/\text{s}$) and results from fast exchange between a free and a bound state. This is in strong contrast to the cases when carboxylic acids are used as sole stabilizer and where slow ligand dynamic (compared to NMR time-scale) exists around the NPs (Figures 5 and S7).

Remarkably, the high temperature ($> 300 \text{ }^\circ\text{C}$) previously reported in the literature for $\text{Ge}(\text{OR})_2$,² and for $(\text{ATI})\text{Ge}(\text{OMe})$ is no more required. The use of this straightforward home-made complex allows decreasing significantly to $160 \text{ }^\circ\text{C}$ which is, to the best of our knowledge, the softest conditions ever reported in the case of thermolytic reduction of germanium species.² Undoubtedly, the more strained ring can be invoked to account for the high reactivity of this new precursor. In contrast to **1** for which acidic proton was necessary to allow decoordination of the ATI ligand, the thermal activation is sufficient to allow NPs formation. Interestingly, the use of a larger variety of ligands system (amines, carboxylic acids, trioctylphosphine) is now possible opening up new perspectives (Figures S8 and S9).

Conclusions

This article outlines, in the context of the challenging synthesis of Ge NPs, the central role of the design of molecular precursors in the pursuit of controlled synthesis in soft conditions. In contrast to the reported pathways which are often based on commercial Ge sources and requires drastic conditions (strong reducing reagents or temperature higher than $300 \text{ }^\circ\text{C}$), we have shown that a proper choice of substituents/ligands on the metal allows softening significantly the experimental conditions (temperature reaction of $160 \text{ }^\circ\text{C}$ in the presence of various stabilizing agents) while keeping physical and structural characteristics. This was achieved thanks to mechanistic studies of the decomposition route of the molecular precursors. Identification of the features responsible of the robustness were identified and modified for developing a low temperature thermolysis pathway. While this strategy is well-established for transition metal species and oxides,³¹ this approach lies far behind in the case of main group metals.³² This works, thus, paves the way to the rational design of molecular precursor as a promising strategy for tackling challenges in the chemistry of nanocrystals involving main group elements.

Acknowledgements

This work was supported by the Université Paul Sabatier, the Région Midi-Pyrénées, the CNRS, the Institut National des Sciences Appliquées of Toulouse, the European Commission for the POCTEFA Interreg project (MET-NANO EFA17/08) and the ANR-08-BLAN-0105-01. D.M. is grateful to the Ministère de l'Enseignement Supérieur et de la Recherche for fellowships, and A.C. is grateful to the Spanish Ministerio de Ciencia e Innovación for a postdoctoral grant. We thank Yannick Coppel and Christian Bijani for NMR measurements, Corinne Routaboul for Raman measurements.

Notes and references

^a Université de Toulouse, UPS, LHFA (Laboratoire Hétérochimie Fondamentale et Appliquée), UMR/CNRS 5069, 118, Route de Narbonne, 31062 Toulouse Cedex 09, France.

^b Université de Toulouse; INSA, UPS, CNRS; LPCNO (Laboratoire de Physique et Chimie des Nano-Objets), 135 avenue de Rangueil, F-31077 Toulouse, France.

^c Institut des Sciences Analytiques et de Physico-Chimie pour l'Environnement et les Matériaux, Université de Pau et des Pays de l'Adour, Hélioparc, 2 av. Président Angot, F-64053 Pau, France.

^d CNRS, LCC (Laboratoire de Chimie de Coordination), 205 route de Narbonne, BP 44099, F-31077 Toulouse Cedex 4, France; Université de Toulouse, UPS, INPT, F-31077 Toulouse Cedex 4, France.

† Electronic Supplementary Information (ESI) available: TGA analysis of the precursors **1-3**, TEM image of germanium NPs prepared from **1** at $320 \text{ }^\circ\text{C}$ in the absence of oleic acid, EDX characterization of Ge/GeO_2 NPs prepared from **1**, ^1H NMR spectrum of the reaction between **1** and carboxylic acid, monitoring of the thermolysis of **1** at $320 \text{ }^\circ\text{C}$ in the presence of oleic acid using UV-Vis spectroscopy, Raman, UV-Vis, photoluminescence of Ge/GeO_2 NPs prepared from **3** at $160 \text{ }^\circ\text{C}$, Raman, DOSY spectrum and TEM images of Ge/GeO_2 NPs prepared from **3** at $320 \text{ }^\circ\text{C}$, TEM images of germanium NPs prepared from **3** at $160 \text{ }^\circ\text{C}$ in the presence of various ligands, HRTEM images of germanium NPs prepared from **3** at $320 \text{ }^\circ\text{C}$. See DOI: 10.1039/b000000x/

- 1 D. V. Talapin, J.-S. Lee, M. V. Kovalenko, E. V. Shevchenko, *Chem. Rev.* 2010, **110**, 389-458.
- 2 D. D. Vaughn, R. E. Schaak, *Chem. Soc. Rev.* 2013, **42**, 2861-2879.
- 3 D. J. Xue, J. J. Wang, Y. Q. Wang, S. Xin, Y. G. Guo, L. J. Wan, *Adv. Mater.* 2011, **23**, 3704-3707.
- 4 H. Gerung, S. D. Bunge, T. J. Boyle, C. J. Brinker, S. M. Han, *Chem. Commun.* 2005, 1914-1916.
- 5 K. Sanderson, *Nature* 2009, 459, 760-761.
- 6 H. Zhu, A. Prakash, D. N. Benoit, C. J. Jones, V. L. Colvin, *Nanotechnology* 2010, **21**, 255604.
- 7 A. Cros-Gagneux, F. Delpech, C. Nayral, A. Cornejo, Y. Coppel, B. Chaudret, *J. Am. Chem. Soc.* 2010, **132**, 18147-18157; H. Virieux, M. Le Troedec, A. Cros-Gagneux, W.-S. Ojo, F. Delpech, C. Nayral, H. Martinez, B. Chaudret, *J. Am. Chem. Soc.* 2012, **134**, 19701-19708.
- 8 D. C. Lee, J. M. Pietryga, I. Robbel, D. J. Werder, R. D. Schaller, V. I. Klimov, *J. Am. Chem. Soc.* 2009, **131**, 3436-3437.
- 9 H. Gerung, T. J. Boyle, L. J. Tribby, S. D. Bunge, C. J. Brinker, S. M. Han, *J. Am. Chem. Soc.* 2006, **128**, 5244-5250.
- 10 W.-S. Ojo, S. Xu, F. Delpech, C. Nayral, B. Chaudret, *Angew. Chem. Int. Ed.* 2012, **51**, 738-741.
- 11 B. K. Hugues, J. M. Luther, M. C. Beard, *ACS Nano* 2012, **6**, 4573-4579.
- 12 T. J. Boyle, L. J. Tribby, L. A. Ottley, S. M. Han, *Eur. J. Inorg. Chem.* 2009, **36**, 5550-5560.
- 13 H. V. R. Dias, Z. Wang, W. Jin, *Coord. Chem. Rev.* 1998, **176**, 67-86; M. Asay, C. Jones, M. Driess, *Chem. Rev.* 2011, **111**, 354-396.
- 14 J. C. Baldwin, M. F. Lappert, J. B. Pedley, J. S. Poland *J. Chem. Soc., Dalton Trans* 1972, 1943-1947; P. Rivière, M. Rivière-Baudet, J. Satgé, in *Comprehensive Organometallic Chemistry*, Vol. 2 (Eds: G. Wilkinson, F. G. A. Stone), Pergamon press, New York, 1982, pp. 399-518.
- 15 H. V. R. Dias, Z. Wang, *J. Am. Chem. Soc.* 1997, **119**, 4650-4655; S. Sinhababu, R. K. Siwatch, G. Mukherjee, G. Rajaraman, S. Nagendran, *Inorg. Chem.* 2012, **51**, 9240-9248.
- 16 K. M. Baines, W. G. Stibbs, *Coord. Chem. Rev.* 1995, **145**, 157-200; M. Veith, A. Rammo, *Z. Anorg. Allg. Chem.* 2001, **627**, 662-668; A. Jana, H. W. Roesky, C. Schulzke, P. P. Samuel, A. Döring, *Inorg. Chem.* 2010, **49**, 5554-5559; S. S. Sen, D. Kratzert, D. Stern, H. W. Roesky, D. Stalke, *Inorg. Chem.* 2010, **49**, 5786-5788; R. K. Siwatch, S. Kundu, D. Kumar, S. Nagendran, *Organometallics* 2011, **30**, 1998-2005; P. P. Samuel, A. P. Singh, S. P. Sarish, J. Matussek, I. Objartel, H. W. Roesky, D. Stalke, *Inorg. Chem.* 2013, **52**, 1544-1549; E. Ballester-Martinez, J. Klosin, B. D. Fahlman, L. W. Pineda, *Eur. J. Inorg. Chem.* 2014, 5233-5239.
- 17 P. Jutzi, S. Keitemeyer, B. Neumann, H. G. Stammer, *Organometallics* 1999, **18**, 4778-4784; L. W. Pineda, V. Jancik, J. F. Colunga-Valladares, H. W. Roesky, A. Hofmeister, J. Magull, *Organometallics* 2006, **25**, 2381-2383.
- 18 A. Kailer, K. G. Nickel, Y. G. Gogotsi, *J. Raman Spectrosc.* 1999, **30**, 939-946.

- 19 M. Ardyanian, H. Rinnert, X. Devaux, M. Vergnat, *Appl. Phys. Lett.* 2006, **89**, 011902.
- 20 M. Micoulaut, L. Cormier, G. S. Henderson, *J. Phys. Condens. Mater.* 2006, **18**, R753-R784.
- 21 E. J. Henderson, C. M. Hessel, J. G. C. Veinot, *J. Am. Chem. Soc.* 2008, **130**, 3624-3632.
- 22 Y. Yin, A. P. Alivisatos, *Nature* 2005, **437**, 664-670.
- 23 C. Bullen, P. Mulvaney, *Langmuir* 2006, **22**, 3007-3013.
- 24 N. El Hawi, C. Nayral, F. Delpéch, Y. Coppel, A. Cornejo, A. Castel, B. Chaudret, *Langmuir* 2009, 7540-7546.
- 25 C. Pan, C. Pelzer, K. Philippot, B. Chaudret, F. Dassenoy, P. Lecante, M. Casanove, *J. Am. Chem. Soc.* 2001, **123**, 7584-7593.
- 26 I. Moreels, J. C. Martins, Z. Hens, *ChemPhysChem* 2006, **7**, 1028-1031.
- 27 L.-M. Lacroix, S. Lachaize, A. Falqui, M. Respaud, B. Chaudret, *J. Am. Chem. Soc.* 2009, **131**, 549-557.
- 28 F. Delpéch, I. A. Guzei, R. F. Jordan, *Organometallics* 2002, **21**, 1167-1176.
- 29 S. Dagorne, D. A. Atwood *Chem. Rev.* 2008, **108**, 4037-4071.
- 30 D. Matioszek, N. Katir, N. Saffon, A. Castel, *Organometallics* 2010, **29**, 3039-3046.
- 31 C. Amiens, B. Chaudret, D. Ciuculescu-Pradines, V. Colliere, K. Fajerweg, P. Fau, M. Kahn, A. Maisonnat, K. Soulantica, K. Philippot, *New J. Chem.* 2013, **37**, 3374-3401. G. A. Seisenbaeva, V. G. Kessler *Nanoscale* 2014, **6**, 6229-6244.
- 32 M. A. Malik, M. Afzaal, P. O'Brien, *Chem. Rev.* 2010, **110**, 4417-4446.
- 33 G. M. Sheldrick, SHELXL-97, Program for Crystal Structure Refinement 1997, University of Göttingen.
- 34 G. M. Sheldrick, *Acta Crystallogr.* 2008, **A64**, 112-122.

ARTICLE

Table of Contents (TOC)

From rational design of organometallic precursors to optimized synthesis of core/shell Ge/GeO₂ nanoparticles

D. Matioszek,^a W.-S. Ojo,^b A. Cornejo,^b . Katir,^a M. El Ezzi,^a M. Le Troedec,^c H. Martinez,^c H. Gornitzka,^d A. Castel,^a C. Nayral,^b and F. Delpech^{b*}

The synthesis conditions of germanium-based nanoparticles have been drastically softened thanks to the design of proper precursor featuring enhanced reactivity.

